DOI: 10.6060/ivkkt.20256804.7164

УДК: 535.37

ПОЛУЧЕНИЕ И ЛЮМИНЕСЦЕНТНЫЕ СВОЙСТВА НЕ СОДЕРЖАЩИХ СВИНЦА ГАЛОГЕНИДНЫХ ДВОЙНЫХ ПЕРОВСКИТНЫХ МАТЕРИАЛОВ

Цзин Сяолун, Лан Тинчан, Т.Г. Черкасова, Хан Тао

Цзинь Сяолун (ORCID 0000-0003-1391-4285)

Школа наук о материалах и инженерии, Чунцинский университет искусств и наук, Чунцин 402160, Китай
Кузбасский государственный технический университет им. Т.Ф. Горбачева, ул. Весенняя, 28, Кемерово, Российская Федерация, 650000
E-mail: jxly1988@163.com

Лан Тинчан (ORCID0000-0002-7867-3307)

Школа наук о материалах и инженерии, Чунцинский университет искусств и наук, Чунцин 402160, Китай
E-mail: 394340508@qq.com

Татьяна Григорьевна Черкасова (ORCID 0000-0002-5337-1337)*

Кузбасский государственный технический университет им. Т.Ф. Горбачева, ул. Весенняя, 28, Кемерово, Российская Федерация, 650000
E-mail: ctg.htnv@kuzstu.ru*

Хан Тао (ORCID 0000-0002-7396-1676)

Колледж материалов и новой энергии, Чунцин 401331, Китай
E-mail: 42507706@qq.com

Известно, что галогенидный перовскит $APbX_3$ ($A = CH_3NH_3^+$, Cs^+; X – ион галогена) является перспективным материалом с интересными фотоэлектрическими и оптоэлектронными свойствами благодаря своим характеристикам переноса заряда, узкополосному излучению, регулируемой длине волны излучения и высокой подвижности носителей. Однако, по причине неблагоприятных факторов, таких как токсичность и легкость разложения перовскита, содержащего галогениды свинца, его исследование и применение ограничены. Для преодоления токсичности и легкости разложения галогенидного перовскита, в этой работе подготовлен методом осаждения материал состава $Cs_2NaBiCl_6$:x%Mn^{2+} (x = 0, 1, 3, 6, 9), где ионы Na^+ и Bi^{3+} заменяют два иона Pb^{2+}, а матрица бессвинцового галогенидного двойного перовскита ($Cs_2NaBiCl_6$) легирована Mn^{2+}. Изучено влияние легирования ионами Mn^{2+} различных концентраций на люминесцентные свойства полученного относительно чистого, не имеющего других гетерофаз материала. Когда содержание ионов Mn^{2+} достигает 6%, интенсивность люминесценции самая высокая. Различные длины волн возбуждения (340 нм, 363 нм, 380 нм) и длины волн испускания (560 нм, 582 нм, 600 нм) использовались для измерения состояния испускания и возбужденного состояния подготовленного образца. Рассчитанные цветовые координаты (0,5288, 0,4665) принадлежат оранжево-желтой области. Результаты работы показывают, что получен неорганический галогенидный двойной перовскитный материал с большими перспективами развития.

Ключевые слова: бессвинцовый галогенидный двойной перовскит, метод осаждения, $Cs_2NaBiCl_6$, оранжево-желтая люминесценция

Для цитирования:
Цзин Сяолун, Лан Тинчан, Черкасова Т.Г., Хан Тао Получение и люминесцентные свойства не содержащих свинца галогенидных двойных перовскитных материалов. *Изв. вузов. Химия и хим. технология*. 2025. Т. 68. Вып. 4. С. 67–72. DOI: 10.6060/ivkkt.20256804.7164.

For citation:
Jing Xiaolong, Lang Tianchun, Cherkasova T.G., Han Tao Preparation and luminescent properties of lead-free halide double perovskite materials. *ChemChemTech* [*Izv. Vyssh. Uchebn. Zaved. Khim. Khim. Tekhnol*.]. 2025. V. 68. N 4. P. 67–72. DOI: 10.6060/ivkkt.20256804.7164.

PREPARATION AND LUMINESCENT PROPERTIES OF LEAD-FREE HALIDE DOUBLE PEROVSKITE MATERIALS

Jing Xiaolong, Lang Tianchun, T.G. Cherkasova, Han Tao

Jing Xiaolong (ORCID 0000-0003-1391-4285)

School of Materials Science and Engineering, Chongqing University of Arts and Sciences, Chongqing 402160, China
T.F. Gorbachev Kuzbass State Technical University, Vesennyaya st., 28, Kemerovo, 650000, Russia
E-mail: jxly1988@163.com

Lang Tianchun (ORCID0000-0002-7867-3307)

School of Materials Science and Engineering, Chongqing University of Arts and Sciences, Chongqing 402160, China
E-mail: 394340508@qq.com

Tatiana G. Cherkasova (ORCID 0000-0002-5337-1337)*

T.F. Gorbachev Kuzbass State Technical University, Vesennyaya st., 28, Kemerovo, 650000, Russia
E-mail: ctg.htnv@kuzstu.ru*

Han Tao (ORCID 0000-0002-7396-1676)

College of Materials and New Energy, Chongqing University of Sciences and Technology, Chongqing 401331, China
E-mail: 42507706@qq.com

Halide perovskite $APbX_3$ ($A = CH_3NH_3^+$, Cs^+; X is a halogen ion) has been proved by scholars to be a material with great potential in photovoltaic and optoelectronic applications due to its charge transport characteristics, narrow-band emission, adjustable emission wavelength and high carrier mobility. However, due to adverse factors such as toxicity and easy decomposition of lead halide perovskite materials, its future development and research application are limited. In order to overcome the toxicity and easy decomposition of halide perovskite, this paper prepared $Cs_2NaBiCl_6$:x%Mn^{2+} (x = 0, 1, 3, 6, 9) by precipitation method. Na^+ and Bi^{3+} ions are substituted two Pb^{2+} ions, and the lead-free halide double perovskite ($Cs_2NaBiCl_6$) matrix was prepared and doped with Mn^{2+}. The effects of different Mn^{2+} doping concentrations on its luminescence properties were studied. The results showed that the prepared sample was relatively pure and there were no other hetero-phase. When the doping concentration of Mn^{2+} reaches 6%, the luminescence intensity is the highest. Different excitation wavelengths (340 nm, 363 nm, 380 nm) and emission wavelengths (560 nm, 582 nm, 600 nm) were used to measure the emission state and excited state of the sample, which showed that the prepared sample was the same emission source. The calculated color coordinates are (0.5288, 0.4665), belonging to the orange-yellow region. Finally, the inorganic halide double perovskite material with great development prospect was obtained.

Keywords: lead-free halide double perovskite, precipitation method, $Cs_2NaBiCl_6$, orange-yellow luminescence

INTRODUCTION

Halide perovskite $APbX_3$ ($A = CH_3NH^{3+}$, Cs^+; X is a halogen ion) has been proved by scholars to be a material with great potential in photovoltaic and optoelectronic applications due to its charge transport characteristics, narrow-band emission, adjustable emission wavelength and high carrier mobility [1-6]. However, due to adverse factors such as toxicity and easy decomposition of lead halide perovskite materials, its future development and research application are limited [7-11]. In order to effectively solve the problems encountered at present, a new type of perovskite with strong stability and no lead is developed to replace the traditional lead halide perovskite materials.

The researchers found that the total inorganic halide double perovskite structure $A_2M_IM_{II}X_6$ ($A = Cs^+$, K^+; $M_I = Ag^+$, K^+, Na^+, Li^+; $M_{II} = Bi^{3+}$, Sb^{3+}, In^{3+}; $X = C1^-$, Br^-, I^- [12-15]. Compared with the traditional

AMX_3 perovskite material, the all-inorganic halide double perovskite material is better in terms of stability and photoelectric performance, and the double perovskite usually does not contain toxic lead elements [16-20]. In addition, its band gap width is relatively narrow, and its absorption rate of ultraviolet light is higher, so it can be better applied in photoelectric devices [21-27]. This alternative method can effectively solve the toxicity and instability of traditional lead halide perovskite materials.

In this paper, Na^+ and Bi^{3+} were selected to replace two Pb^{2+} ions, and the lead-free halide double perovskite ($Cs_2NaBiCl_6$) matrix was prepared and doped with Mn^{2+}. By adjusting the doping concentration of Mn^{2+}, a series of characteristics were carried out on its phase, luminescence properties, micro-morphology and element composition. Finally, the inorganic halide double perovskite material with great development prospect was obtained.

EXPERIMENT AND CHARACTERIZATION

The samples of $Cs_2NaBiCl_6$:x%Mn^{2+} (x = 0, 1, 3, 6, 9) were synthesized by precipitation method, the required drugs were accurately weighed according to the stoichiometric ratio, 3 mmol $BiCl_6$, 3 mmol NaCl, 6 mmol CsCl and corresponding doping ratio of $MnCl_2 \cdot 4H_2O$ were put into a beaker, stir, add 12 ml HCl, stir for a certain period of time, pump and filter, rinse the beaker with anhydrous ethanol, and then put it into a 70 °C air drying box for about 4 h. Finally get the required sample.

In order to characterize the relevant properties of the samples, TD-3500 X-ray diffractometer (XRD) was used to measure the $Cs_2NaBiCl_6$:6%Mn^{2+} sample, which is the most luminous, with an operating voltage of 30 kV, a current of 20 mA, and a test Angle range of 10-70°. The emission and excitation spectra of $Cs_2NaBiCl_6$:x%Mn^{2+} (x = 0, 1, 3, 6, 9) samples were measured by the Hitachi F-7000 fluorescence spectrophotometer at different excitation wavelengths and emission wavelengths. The GeminiSEM 300 field emission scanning electron microscope (SEM) was used to observe the microstructure of the sample and analyze the elemental composition of the sample.

RESULTS AND DISCUSSION

$Cs_2NaBiCl_6$ has a typical face-centered cubic structure, with alternating combinations of $[NaCl_6]^{5-}$ octahedrons and $[BiCl_6]^{3-}$ octahedrons forming a stereo-structure. According to the principle of similar electric neutrality and ionic radius, doped Mn^{2+} will replace the site of Bi^{3+} to form $[MnCl_6]^{4-}$. Fig. 1 shows the XRD pattern of $Cs_2NaBiCl_6$:6%Mn^{2+}. The upper curve is the pattern of the measured sample, and the black line at the bottom is the standard PDF 05-9059 card of $Cs_2NaBiCl_6$. It can be found that each measured peak is aligned with the standard one. In summary, it is shown that the prepared sample phase structure is consistent with the expected, the material is relatively pure, and there are no other impurity phases.

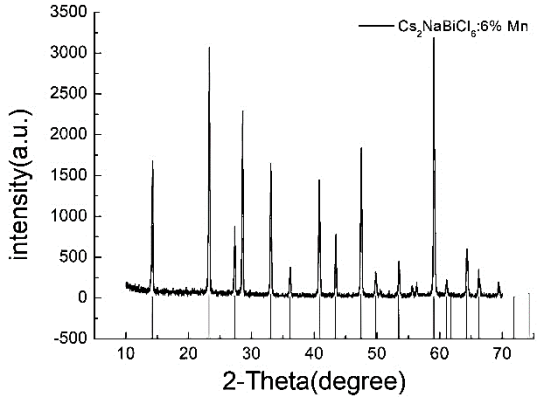

Fig. 1. X-ray diffraction pattern of $Cs_2NaBiCl_6$:6%Mn^{2+}
Рис. 1. Дифрактограмма $Cs_2NaBiCl_6$:6%Mn^{2+}

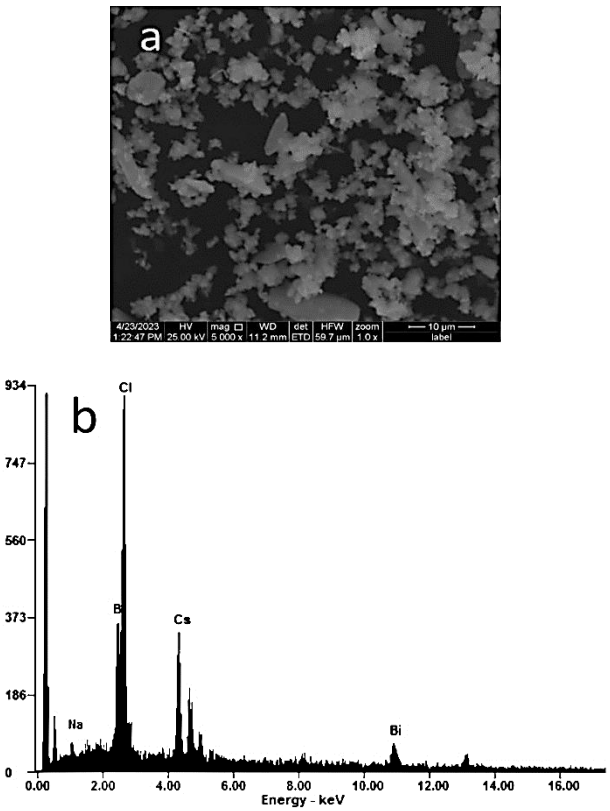

Fig. 2. SEM (a) and EDS (b) spectra of $Cs_2NaBiCl_6$:6%Mn^{2+}
Рис. 2. Спектры СЭМ (а) и ЭДС (б) $Cs_2NaBiCl_6$:6%Mn^{2+}

The morphology of $Cs_2NaBiCl_6$:6%Mn^{2+} was observed under scanning electron microscope. As shown in Fig. 2 (left), the double perovskite sample prepared by precipitation showed uneven microstructure. In addition, EDS spectra of $Cs_2NaBiCl_6$:6%Mn^{2+}

samples were also analyzed, as shown in Fig. 2 (right). The detection shows that between 0-1 kV, the first two peaks are carbon and oxygen, which are the elements contained in the conductive adhesive used in the preparation of the test sample. The elements corresponding to the subsequent wave peaks are corresponding to the elements required for sample preparation, among which, due to the low doping content of manganese, they are not shown in the energy spectrum. In summary, the elements of the measured samples are basically consistent with the designed and prepared samples.

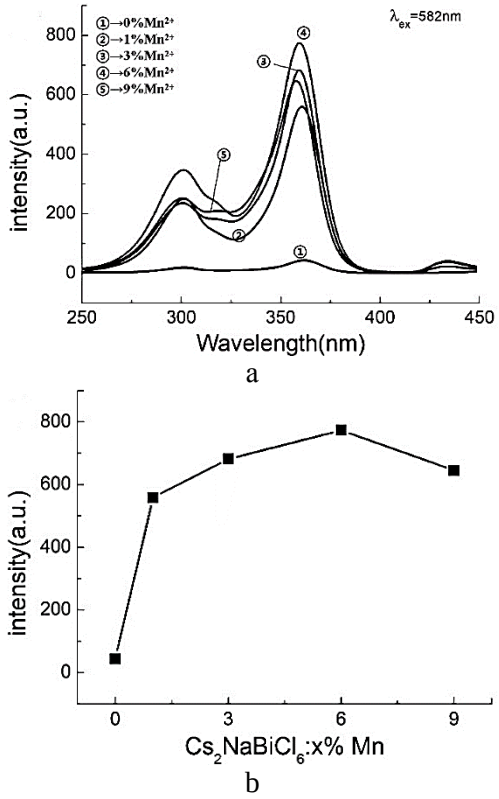

Fig. 3. The excitation spectrum of $Cs_2NaBiCl_6$: x% Mn^{2+}(x = 0, 1, 3, 6, 9) when the emission wavelength is 582 nm (a); the luminous intensity of different doping concentrations at the same emission wavelength (b)

Рис. 3. Спектр возбуждения $Cs_2NaBiCl_6$:x%Mn^{2+}(x = 0, 1, 3, 6, 9) при длине волны излучения 582 нм (a); интенсивность свечения при различных концентрациях легирующего вещества при одной и той же длине волны излучения (b)

$Cs_2NaBiCl_6$ is a standard cubic phase crystal structure with a wide direct band gap. As shown in Fig. 3a, the excitation spectra obtained when the monitoring wavelength is 582 nm, it can be found that $Cs_2NaBiCl_6$ fluorescent materials with different doping concentrations of manganese ions have a main absorption peak centered on the wavelength of 363 nm. As shown in Fig. 3b, the excitation spectral intensity is relatively close when the doping concentration of manganese ions reaches 6%. The excitation spectral intensity reached the highest, and then the luminescence intensity gradually decreased with the increase of doping concentration.

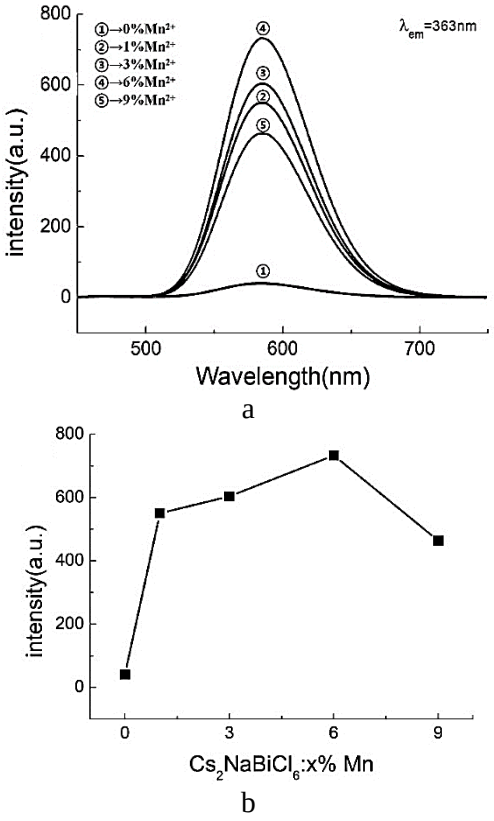

Fig. 4. The emission spectrum of $Cs_2NaBiCl_6$:x%Mn^{2+}(x = 0, 1, 3,
Fig. 4. The exitation spectrum of $Cs_2NaBiCl_6$:x%Mn^{2+}(x = 0, 1, 3, 6, 9) with an excitation wavelength of 336 nm (a); the luminous intensity of different doping concentrations at the same excitation wavelength (b)

Рис. 4. Спектр излучения $Cs_2NaBiCl_6$:x%Mn^{2+}(x = 0, 1, 3, 6, 9) при длине волны возбуждения 336 нм (a); интенсивность свечения при различных концентрациях легирующего вещества при одной и той же длине волны возбуждения (b)

Fig. 4a shows the emission spectrum of $Cs_2NaBiCl_6$:x%Mn^{2+}(x = 0, 1, 3, 6, 9) fluorescent material at an excitation wavelength of 336 nm. It can be seen from the figure that the undoped $Cs_2NaBiCl_6$ matrix has a very low luminous intensity and almost no absorption peak. This is in line with the fact that the inherent parity transition prohibition with double perovskites results in low luminous efficiency [27]. With the continuous increase of manganese ion doping concentration, its luminous intensity first increases and then decreases. When the doping ratio reaches 6%, the luminous intensity reaches the maximum as shown in Fig. 4b. This emission band is due to the doping of manganese ions, which breaks the parity forbidden transition, and the d orbital of manganese ions has an energy level transition from $^4T_1$ to $^6A_1$ [28], which also

produces a relatively obvious orange-yellow photoluminescence.

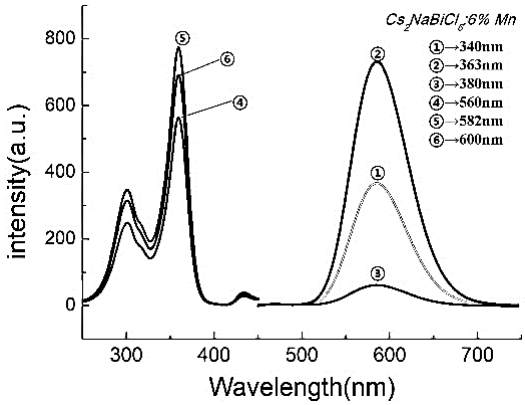

Fig. 5. Spectra of $Cs_2NaBiCl_6$:6%Mn^{2+} at different excitation and emission wavelengths

Рис. 5. Спектры $Cs_2NaBiCl_6$:6%Mn^{2+} при различных длинах волн возбуждения и излучения

Different excitation wavelengths (340 nm, 363 nm, 380 nm) and emission wavelengths (560 nm, 582 nm, 600 nm) were used to measure the emission state and excited state of the sample (as shown in Fig. 5), and it was found that the excitation spectrum and emission spectrum were not offset, indicating that the prepared sample was the same emission source.

All the prepared samples were placed under the three-purpose ultraviolet analyzer for preliminary observation as shown in Fig 6a. It was observed that the samples with different doping concentrations showed different intensity of orange-yellow light at 254 nm and visible light, but the luminous intensity was stronger in visible light mode. The color coordinates of the data measured in the excitation spectrum are added to the analysis system, and the color coordinates obtained from the calculation plot (0.5288, 0.4665) are also in the orange-yellow region, as shown in Fig. 6b.

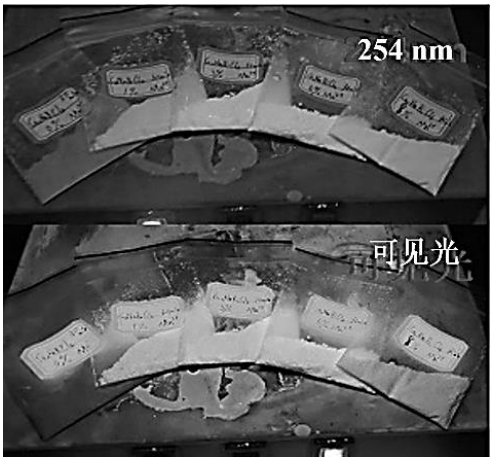

a

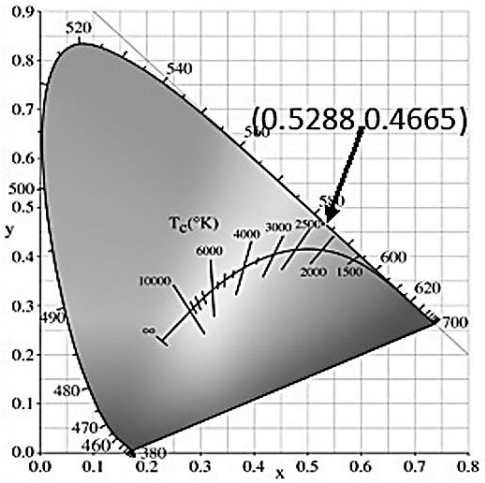

b

Fig. 6. Photos and coordinate analysis diagram of $Cs_2NaBiCl_6$:x%Mn^{2+} under ultraviolet analyzer

Рис. 6. Фотографии и схема анализа координат $Cs_2NaBiCl_6$:x%Mn^{2+} в ультрафиолетовом анализаторе

CONCLUSION

In this paper, a series of $Cs_2NaBiCl_6$:x% Mn^{2+}(x = 0, 1, 3, 6, 9) double perovskite fluorescence materials were prepared and synthesized by precipitation method [29, 30]. Through the characterization of various instruments and the analysis of data, it was found that the obtained sample phase is pure and almost free of other impurities. The obtained samples are basically consistent with the elements of the experimental design. The luminescence of the sample comes from the same excitation source. With the increase of manganese ion doping concentration, the luminous intensity of the sample increases, reaching the highest at 6%, and showing a strong orange-yellow light, but with the increase of Mn^{2+} doping concentration, due to the concentration quenching effect, the intensity decreases. The preparation method has the advantages of simple process, low raw material cost, short reaction time and pure material ratio. Therefore, $Cs_2NaBiCl_6$: x% Mn^{2+} fluorescent materials have great application potential in the preparation of LED devices and luminous display agents.

The authors declare the absence of a conflict of interest warranting disclosure in this article.

Авторы заявляют об отсутствии конфликта интересов, требующего раскрытия в данной статье.

REFERENCES
ЛИТЕРАТУРА

1. **Nangha N.K., Nag A.** Synthesis and luminescence of Mn-doped $Cs_2AgInCl_6$ double perovskites. *Chem Commun (Camb).* 2018. V. 54. N 41. P. 5205-5208. DOI: 10.1021/acsomega.0c04599.
2. **Xu Qiyuan.** Preparation and luminescence properties of rare earth doped phosphate fluorescent materials. *Changchun Univ. Sci. Technol.* 2022. P. 000328. DOI: 10.1016/j.gsf.2020.04.013.
3. **Fan Xiaoyi.** Preparation and properties of rare earth ion doped boron/phosphate luminescent materials. *Central South University of Forestry and Technology*. 2021. P. 000062. DOI: 10.27662/d.cnki.gznlc.2020.000082.
4. **Lu C.H., Biesold-Mcgee G.V., Liu Y.** Doping and ion substitution in colloidal metal halide perovskite nanocrystals. *Chem. Soc. Rev.* 2020. V. 49. N 14. P. 4953-5007. DOI: 10.1039/C9CS00790C.
5. **Green M.A., Ho-Baillie A., Snaith H.J.** The emergence of perovskite solar cells. *Nature Photonics.* 2014. V. 8. N 7. P. 506-514. DOI: 10.1038/nphoton.2014.134.
6. **Zhao X.G., Yang J.H., Fu Y.** Design of Lead-Free Inorganic Halide Perovskites for Solar Cells via Cation-Transmutation. *J. Am. Chem. Soc.* 2017. V. 139. N 7. P. 2630-2638. DOI: 10.1021/jacs.6b09645.
7. **Liu C., Yang Y., Liu X.** Quasi-quantum dot-induced stabilization of α-$CsPbI_3$ perovskite for high-efficiency solar cells. *J. Mater. Chem. A.* 2020. V. 8. N 20. P. 10226-10232. DOI: 10.1039/D0TA02807J.
8. **Li F., Xia Z., Pan C.** High Br-Content $CsPb(Cl_yBr_{1-y})_3$ Perovskite Nanocrystals with Strong Mn^{2+} Emission through Diverse Cation/Anion Exchange Engineering. *ACS Appl. Mater. Interfaces*. 2018. V. 10. N 14. P. 11739-11746. DOI: 10.1021/acsnano.6b07574.
9. **Snaith H J.** Present status and future prospects of perovskite photovoltaics. *Nature Mater*. 2018. V. 17. N 5. P. 372-376. DOI: 10.1038/s41563-018-0071-z.
10. **Berri S., Bouarissa N.** Ab initio study of fundamental properties of $ACdX_3$(A= K, Rb, Cs; and X= F, Cl, Br) halide perovskite compounds. *Emergent Mater.* 2023. V. 6. N 3. P. 1009-1025. DOI: 10.1002/pssb.202300280.
11. **Mingchao Wang, Vallabh Vasudevan, Shangchao Lin.** Molecular mechanisms of thermal instability in hybrid perovskite light absorbers for photovoltaic solar cells. *J. Mater. Chem. A.* 2020. V. 8. P. 17765-17779. DOI: 10.1039/d0ta05356.
12. **Zhang P., Yang J., Wei S.-H.** Manipulation of cation combinations and configurations of halide double perovskites for solar cell absorbers. *J. Mater. Chem. A.* 2018. V. 6. N 4. P. 1809-1815. DOI: 10.1039/C7TA09713A.
13. **Meyer E., Mutukwa D., Zingwe N.** Lead-free halide double perovskites: a review of the structural, optical, and stability properties as well as their viability to replace lead halide perovskites. *Metals.* 2018. V. 8. N 9. P. 667. DOI: 10.3390/met8090667.
14. **Ou T J, Zhuang Q, Yan H C, Feng S, Li P F, Ma X J.** Lead-free halide double perovskites Rb_2InSbX_6(X= F, Cl, Br, I): A first-principles study of structural and optoelectrical properties. *Chem. Phys.* 2023. V. 573. P. 112015. DOI: 10.1016/j.chemphys.2023.112015.
15. **Lavadiya S., Ahmed M.S., Barman C.** Temperature-Dependent Structure–Property Relationship of Mn-Doped $Cs_2AgInCl_6$ Thin Films Impacts Its Application as a Self-Powered UV Photodetector. *ACS Appl. Electronic Mater.* 2024. V. 6. N 4. P. 2749-2758. DOI: 10.1021/acsaelm.3c00563.
16. **Boutramine A., Al-Qaisi S., Samah S.** Optoelectronic and thermoelectric properties of new lead-free K2NaSbZ6 (Z= Br, I) halide double-perovskites for clean energy applications: a DFT study. *Opt. Quantum Electron*. 2024. V. 56. N 3. P. 417. DOI: 10.1007/s1182-024-063344-4.
17. **Mustafa G.M., Nawaz M.U., Noor N.A.** Lead free A_2NaInI_6 (A= Cs, Rb, K) double perovskites for optoelectronic and thermoelectric applications. *Phys. Scripta*. 2024. V. 99. N 4. P. 045960. DOI: 10.1088/1402-4896/ad32b3.
18. **Tran M., Cleveland I., Geniesse J.** High photoluminescence quantum yield near-infrared emission from a lead-free ytterbium-doped double perovskite. *Mater. Horizons*. 2022. V. 9. N 8. P. 2191-2197. DOI: 10.1039/D2MH00483F.
19. **Tailor N.K., Listorti A., Colella S.** Lead-Free Halide Double Perovskites: Fundamentals, Challenges, and Photovoltaics Applications. *Adv. Mater. Technol.* 2023. V. 8. N 1. P. 2200442. DOI: 10.1002/admt.202200442.
20. **Igbari F., Wang Z.K., Liao L.S.** Progress of Lead-Free Halide Double Perovskites. *Adv. Energy Mater.* 2019. V. 9. N 12. P. 1803150. DOI: 10.1002/aenm.201803150.
21. **McClure E.T., Ball M.R., Windl W.** Cs_2AgBiX_6 (X = Br, Cl) - New visible light absorbing, lead-free halide perovskite semiconductors. *Chem. Mater.* 2016. V. 28. N 5. P. 1348-1354. DOI: 10.1021/acs.chemmater.5b04231.
22. **Zewen Xiao, Weiwei Meng, Jianbo Wang.** Thermodynamic Stability and Defect Chemistry of Bismuth-Based Lead-Free Double Perovskites. *ChemSusChem*. 2016. V. 9. P. 1-7. DOI: 10.1002/cssc.201600679.
23. **Fuxiang Ji, Johan Klarbring, Feng Wang.** Lead-Free Halide Double Perovskite $Cs_2AgBiBr_6$ with Decreased Bandgap. *Angew. Chem.* 2020. V. 132. N 35. P. 15303-15306. DOI: 10.1002/ange.202005568.
24. **Zhang L., Fang Y., Sui L.** Tuning Emission and Electron–Phonon Coupling in Lead-Free Halide Double Perovskite $Cs_2AgBiCl_6$ under Pressure. *ACS Energy Lett.* 2019. V. 4. N 12. P. 2975-2982. DOI: 10.1021/acsenergylett.9b02155.
25. **Zhou J., Xia Z., Molokeev M.S.** Composition design, optical gap and stability investigations of lead-free halide double perovskite $Cs_2AgInCl_6$. *J. Mater. Chem. A.* 2017. V. 5. N 29. P. 15031-15037. DOI: 10.1039/c7ta04690.
26. **Jiajun Luo, Xiaoming Wang, Shunran Li.** Efficient and stable emission of warm-white light from lead-free halide double perovskites. *Nature*. 2018. V. 563. P. 541–545. DOI: 1038/s41586-018-0691-0.
27. **Weiwei Meng, Xiaoming Wang, Zewen Xiao.** Parity-Forbidden Transitions and Their Impact on the Optical Absorption Properties of Lead-Free Metal Halide Perovskites and Double Perovskites. *J. Phys. Chem. Lett.* 2017. V. 8. N 13. P. 2999-3007. DOI: 10.1021/acs.jpclett.7b01042.
28. **Nag A., Chakraborty S., Satma D.D.** To dope Mn^{2+} in a semiconducting nanocrystal. *J. Amer. Chem. Soc.* 2008. V. 130. N 32. P. 10605–10611. DOI: 10.1021/ja801249z.
29. **Filatova N.V., Kosenko N.F., Badanov M.A.** Physico-Chemical study of the behavior of mullite precursor synthesized with co-presipitation. *ChemChemTech [Izv. Vyssh. Uchebn. Zaved. Khim. Khim. Tekhnol.]*. 2021. V. 64. N 11. P. 97-102. **Филатова Н.В., Косенко Н.Ф., Баданов М.А.** Физико-химическое изучение поведения муллитового прекурсора, синтезированного соосаждением. *Изв. вузов. Химия и хим. технология.* 2021. Т. 64. Вып. 11. С. 97-102. DOI: 10.6060/ivkkt.20216411.6478.
30. **Kochergin T.P., Ponomaryova T.S., Goryacheva I.Y.** Production and Properties of a Photoluminescent coating based on semiconductor quantum dots in a hollow core of microstructured glass. *ChemChemTech [Izv. Vyssh. Uchebn. Zaved. Khim. Khim. Tekhnol.]*. 2023. V. 66. N 2. P. 85-91. **Кочергин Т.П., Пономарева Т.С., Горячева И.Ю.** Получение и свойства фотолюминесцентного покрытия на основе полупроводниковых квантовых точек в полой сердцевине микроструктурированного стекла. *Изв. вузов. Химия и хим. технология.* 2023. Т. 66. Вып. 2. С. 85-91. DOI: 10.6060/ivkkt.20236602.6615.

Поступила в редакцию (Received) 07.11.2024
Принята к опубликованию (Accepted) 02.12.2024